Quaternary Research 80 (2013) 235–249

Contents lists available at ScienceDirect

Quaternary Research

journal homepage: www.elsevier.com/locate/yqres

Use of single-grain geochemistry of cryptic tuffs and volcaniclastic sandstones improves the tephrostratigraphic framework of Olduvai Gorge, Tanzania

Lindsay J. McHenry [a,*], Harald Stollhofen [b], Ian G. Stanistreet [c]

[a] Department of Geosciences, University of Wisconsin-Milwaukee, 3209 N. Maryland Ave., Milwaukee, WI 53211, USA
[b] GeoZentrum Nordbayern, Friedrich-Alexander-Universität Erlangen-Nürnberg (FAU), Schlossgarten 5, 91054 Erlangen, Germany
[c] Dept. of Earth, Ocean and Ecological Sciences, University of Liverpool, Brownlow Street, PO Box 147, Liverpool L69 3GP, UK

A R T I C L E I N F O

Article history:
Received 28 November 2012
Available online 19 June 2013

Keywords:
Olduvai Gorge
Pleistocene
Tephrostratigraphy
Sedimentology

A B S T R A C T

Single-grain geochemical composition of volcaniclastic sandstones can be a potential tool to improve correlations of mixed pyroclastic/epiclastic deposits. To test this, trachytic tuffs of the paleoanthropologically important FLK, FLK N, and FLK NN sites of Pleistocene Olduvai Gorge Bed I (Tanzania) are used as an established tephrostratigraphic framework against which to test volcaniclastic sandstone correlations. Fluvio-lacustrine sandstones and tuff samples were collected from eight archeological trenches between Tuffs IB and ID across a 500-m transect, including Leakey's famous *Zinjanthropus* (FLK) and OH 7/OH 8 (FLK NN) sites. A previously unknown, thin, fine, mineralogically unique, black trachyandesitic fallout ash was discovered below Tuff IC. Compositions of individual augite, feldspar and titanomagnetite grains from sandstones between Tuffs IB and IC reveal some IB-equivalent material, and a new compositional assemblage distinct from the sandwiching marker tuffs. Mineral compositions of the "tripartite" volcaniclastic sandstone between Tuffs IC and ID are similar to ID. Volcaniclastic sandstone grain fingerprints further refine correlations between fluvio-lacustrine sections within the area, providing support for proposed high-resolution stratigraphic reconstruction of the *Zinjanthropus* and OH 7/OH 8 land surfaces. This method might be applied to other sections where pyroclastic particles are admixed but distinct tuffs are not preserved.

Introduction

Tephrostratigraphy is a leading technique for establishing both local and regional stratigraphic frameworks in regions with records of explosive volcanic activity. Identifying an individual tuff (or series of tuffs) at multiple sites can help constrain a time interval that can be used for paleoenvironmental landscape reconstruction at adjacent levels and can substantially support correlations based on physical mapping and individual measured sections and trenches. Large-scale explosive eruptions potentially generate widespread marker tuffs that can be used to correlate over an entire region (e.g., Sarna-Wojcicki, 2000; Sarna-Wojcicki and Davis, 1991; WoldeGabriel et al., 2005; Alloway et al., 2007; Stollhofen et al., 2008a; Lowe, 2011). Local, near-source volcanic records of more frequent, smaller-scale eruptions as well as distal volcanic ash fallout can provide high stratigraphic resolution for limited areas (e.g., McHenry, 2005, 2012), in particular when erupted magma compositions are changing through time. While most tuff "fingerprinting" relies on volcanic glass geochemistry (e.g., Froggatt, 1992; Lowe, 2011), phenocryst compositions can alternatively be used for local tephrostratigraphic correlation where glass is absent or heavily altered (e.g., Cronin et al., 1996; McHenry, 2005; Turner et al., 2009; Matsu'ura et al., 2011; McHenry, 2012).

Reworked volcaniclastic sandstones can also potentially be used for tephrostratigraphy. For example, Tryon et al. (2009) used glass compositions in reworked tephra units to help correlate between Paleolithic sites in Anatolia. The current research builds upon this methodology, applying phenocryst-based geochemical fingerprinting to the mineral components of reworked volcaniclastic sandstones found between primary pyroclastic flow, surge and fallout tuffs at Olduvai Gorge, Tanzania. These sandstones derive from multiple sources, and in some cases they preserve components not observed in the enclosing primary tuffs, potentially providing additional units for fingerprinting and stratigraphic refinement.

Olduvai geology

Olduvai Gorge is located directly adjacent to the Ngorongoro Volcanic Highlands (NVH) of northern Tanzania, and exposes an extensive record of tuffs derived from both major and much smaller eruptions. The volcanic units are interbedded with the Pleistocene fluvio-lacustrine succession of paleolake Olduvai (Hay, 1976). The main Olduvai Bed I tuffs (Fig. 1) have been well documented compositionally and used to create a stratigraphic framework across the 20-km basin (Hay, 1976; McHenry, 2005, 2012). However, this

* Corresponding author.
E-mail address: lmchenry@uwm.edu (L.J. McHenry).

0033-5894/$ – see front matter © 2013 University of Washington. Published by Elsevier Inc. All rights reserved.
http://dx.doi.org/10.1016/j.yqres.2013.05.006

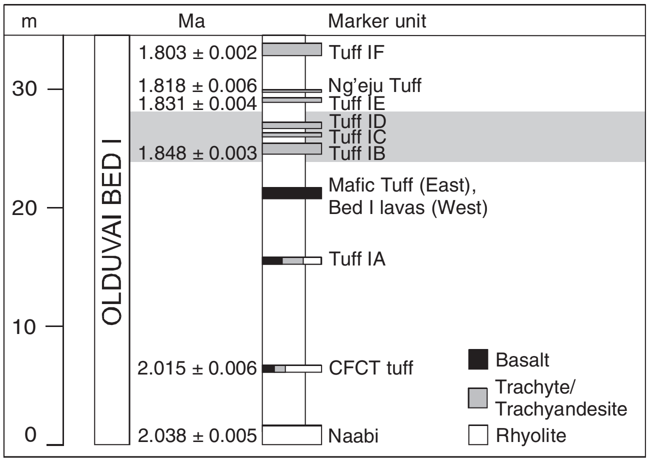

Figure 1. Olduvai Bed I tephrostratigraphy, composite section. Dates from Deino, 2012. The focus of the current study is the interval from Tuff IB to Tuff ID (marked by gray bar) within the upper part of Bed I. At the sites of interest (FLK area) Upper Bed I is underlain by basaltic lavas shortly below the level of Tuff IB; the lower Bed I succession is only exposed in the far western gorge.

framework is sometimes insufficient to support high-resolution correlations at a site-to-site level between localities of paleoanthropological interest, especially when the target is to identify specific hominin exploitation levels, such as the FLK *Zinjanthropus* (*Zinj*) and FLK NN level 3 (OH 7/OH 8) land surfaces. To increase this resolution, it is necessary to consider the mineralogical and geochemical compositions of even minor tuffs and volcaniclastic sandstone grain separates in the intervals between the major marker tuffs that constitute the principal tephrostratigraphic framework. If these differ substantially in composition, it may be possible to use them as additional marker beds to establish an even higher resolution stratigraphic framework.

We have chosen to test this idea in the FLK area (Fig. 2: *Zinjanthropus* Locality 45 (FLK)) and surrounding sites (FLK N, FLK NN, FLK S, FLK Maiko Gully), where there are multiple archeologically and paleontologically rich paleo-land surfaces and sites constrained between marker Tuffs IB, IC, and ID. The Olduvai Landscape Paleoanthropology Project (OLAPP) has systematically excavated fourteen trenches over this stratigraphic interval in the FLK area (Fig. 2), allowing us to collect samples with well-constrained paleoanthropological contexts. Figure 3 illustrates the Tuff IB to Tuff ID section in the back wall of OLAPP Trench 138, excavated 25 m to the northeast of Leakey's (1971) classic FLK *Zinjanthropus* Locality 45.

Objectives

The objectives of this contribution are to: (1) confirm the identification of individual marker units (Tuffs IB, IC, and ID) in the FLK area, using geochemical fingerprints of phenocryst separates established both here and in other areas of the Olduvai Basin (McHenry, 2005, 2012); (2) determine whether the geochemical compositions of detrital grains from volcaniclastic sandstones can be linked to known phenocryst fingerprints of the sandwiching Bed I tuff markers; (3) identify additional "dilute" pyroclastic input only recorded by unique volcaniclastic sandstone grain compositions; (4) test whether these "cryptic" pyroclastic source compositions can be used to characterize a particular volcaniclastic sandstone interval; and (5) apply the newly developed volcaniclastic grain fingerprints to the FLK area sites

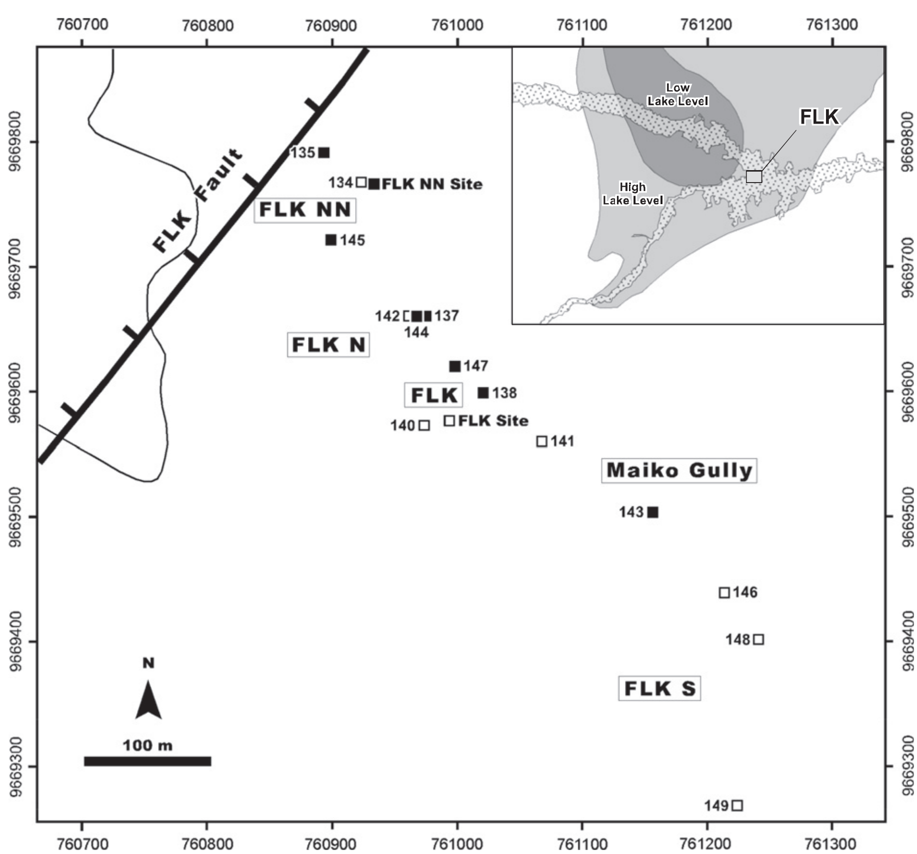

Figure 2. Olduvai Gorge and site maps. Upper inset: map of Olduvai Gorge, showing location of Upper Bed I paleolake and FLK area. Larger map: relative positions of FLK, FLK N, and FLK NN Leakey (1971) locations within the greater FLK area, and locations and numbers of OLAPP trenches. Sampled trenches are marked by black squares; trenches and locations that were not sampled but measured and/or mentioned in the text are marked by open squares.
Maps modified and extended from Blumenschine et al. (2012a).

https://doi.org/10.1016/j.yqres.2013.05.006 Published online by Cambridge University Press

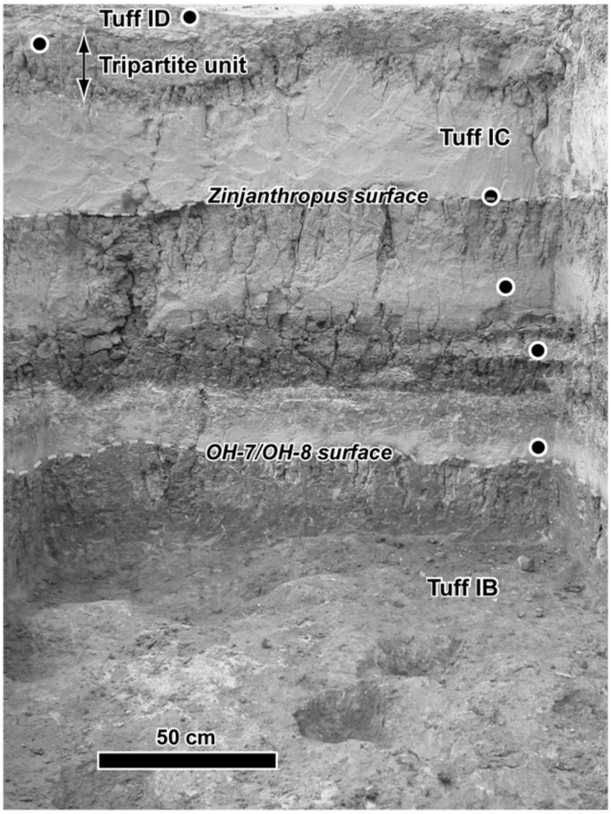

Figure 3. Photograph, showing the Tuff IB to Tuff ID stratigraphic interval exposed in Trench 138 (25 m NE of the classic *Zinjanthropus* Locality 45). Figure 6 provides a measured section of this stratigraphic interval. Note the trampled top surface of Tuff IB and intensive rooting and burrowing associated with the *Zinjanthropus* and OH 7/OH 8 land surfaces. Circles mark sampling points.

to support the results of physical stratigraphic mapping in this paleoanthropologically critical area and interval.

Paleoanthropological background

Olduvai Gorge exposes a record of paleontologically rich Pleistocene sediments interlayered with dominantly trachytic tuffs derived from the adjacent NVH. These tuffs help constrain the stratigraphic positions of many sites of paleoanthropological significance, and within Bed I (the oldest and thickest unit), each of the major marker tuffs has been geochemically fingerprinted using a combination of glass and phenocryst compositions (McHenry, 2005; McHenry et al., 2008; Stollhofen et al., 2008b; McHenry, 2012).

Three of the most studied sites in Bed I at Olduvai Gorge are FLK, FLK N, and FLK NN (Fig. 2), situated in the eastern paleo-lake margin area. FLK (Hay, 1976: Locality 45) includes, Mary Leakey's famous *Zinjanthropus* excavation site (which yielded the *Zinjanthropus* skull, subsequently attributed to *Paranthropus boisei*), while Olduvai Hominins (OH) 7 (the type specimen of *Homo habilis*) and 8 (an articulated foot paratype) were found at FLK NN (Hay, 1976: Locality 45b) slightly to the northwest (Leakey, 1971). Ongoing research by OLAPP provides a high-resolution sequence stratigraphic framework for individual surfaces between these sites (Stanistreet, 2012). Tuffs IB, IC, and ID have been provisionally identified in these strata. Between these tuffs are a series of lacustrine claystones and fluvial volcaniclastic sandstones, along with paleontologically and archeologically rich paleo-land surfaces. The "*Zinjanthropus* surface," beneath Tuff IC, also known as FLK level 22, produced one of the world's richest assemblages of Oldowan stone tools and faunal elements (Leakey, 1971). This surface correlates stratigraphically to FLK NN level 1, excavated by Leakey (1971) 200 m to the northwest of FLK, which yielded some artifacts (n = 34) and vertebrate fossils (n = 275). FLK NN level 3, stratigraphically lower in the same excavation, yielded an abundant and important vertebrate fossil sample (n = 2158), including the OH 7 type specimen of *H. habilis* and OH 8, an articulated foot representing one of this taxon's paratypes. The OH 7/OH 8 land surface, which was rich in vertebrate fossils at the Leakey excavation at FLK NN (level 3) and the nearby OLAPP trench 135, is not especially rich elsewhere in the FLK area.

The close geographic and stratigraphic occurrences of *Zinjanthropus* (representing *P. boisei*) at FLK and OH 7 (type specimen of *H. habilis*) at nearby FLK NN were an early line of evidence that these two species coexisted in time and space at Olduvai (e.g., Leakey, 1971), illustrating the complexity of the hominin record at the site. Their apparent coexistence also complicates the attribution of the contemporary Oldowan lithic technology to a specific hominin species.

The aim of this paper forms part of the ambitions of the Olduvai Landscape and Paleoanthropology Project (OLAPP), seeking to improve on and refine the work of Leakey (1971) and Hay (1976) in Beds I and II at Olduvai by integrating a broad front of scientific disciplines in support of archeological excavations and paleoanthropology. In addition to new chronostratigraphic (Deino, 2012), tephrostratigraphic (McHenry, 2004, 2005; McHenry et al., 2008; McHenry, 2012) and volcanological (Stollhofen et al., 2008b) studies, refinements in sedimentology and stratigraphy (Stanistreet, 2012; Stollhofen and Stanistreet, 2012) and paleobotany (Bamford et al., 2006, 2008; Albert and Bamford, 2012; Bamford, 2012) have allowed more exact paleoenvironmental and paleoecological reconstructions of important hominin levels (Blumenschine et al., 2012a,b; Njau and Blumenschine, 2012). The present paper attempts to build on this endeavor across a disciplinary divide between volcanology and sedimentology, aiming to see to what extent volcaniclastic sandstone components might be geochemically fingerprinted to improve tephrostratigraphic resolution.

Up-to-date interpretations of the paleoenvironments of the Bed I FLK, FLK N, and FLK NN sites place them in the lake margin area of saline-alkaline paleo-lake Olduvai (e.g., Blumenschine et al., 2012a), though the exact nature of the lake margin area during this time (e.g., groundwater or stream-fed wetlands, oasis, hill, or peninsula) is still under debate (cf. Ashley et al., 2010a,b; Blumenschine et al., 2012a). Details of the paleoecological interpretation of the sites using data derived from the same trenches sampled in this study are detailed in Blumenschine et al. (2012a). They reconstruct a landscape involving a small, treed peninsula at FLK separating a fluvial channel to the south and a freshwater wetland to the north. Signs of hominin activity are prevalent at FLK but less so in surrounding areas, suggesting that hominins favored this site, with its trees providing refuge from the sun and predators. Leakey (1971) interpreted this large concentration of faunal remains and stone tools as an "occupation floor," while Blumenschine et al. (2012a) contend that predation risk, evidenced by crocodile (Njau and Blumenschine, 2012) and leopard-like carnivore toothmarks on hominin bones (Pante et al., 2012), would have been too high for long-term occupation, but that the site would have been visited and used frequently to access carcasses and other resources.

Methods

Samples of tuffs and volcaniclastic sandstones were collected from eight OLAPP archeological trenches over the Tuff IB to Tuff ID interval (Fig. 2; Table 1). At least one sample of each tuff (IB, IC, and ID) was collected to compare to the geochemical database of McHenry (2004, 2005, 2012) to confirm that these framework-building marker units had been properly identified in the FLK area. The volcaniclastic nature of sandstones was determined on the basis of the presence of 25–75% pumice, glass shard and compact vitric particles (in this case all altered) in addition to crystals and crystal fragments of feldspar, augite or titanomagnetite. Most are further characterized by the occurrence of mud clasts, other non-volcanic detrital grains and clay matrix.

https://doi.org/10.1016/j.yqres.2013.05.006 Published online by Cambridge University Press

Table 1
Sample localities and descriptions.

Sample	Trench	Locality	Strat position	Description	Composition
07-T2	135	FLK NN	IC-ID	Sandstone	Like ID
07-T3	135	FLK NN	IC-ID	Sandstone lens below 07-T2	Like ID
07-T5	135	FLK NN	IB-IC	Sandstone above 07-T4	HMC
07-T4	135	FLK NN	IB-IC	Sandstone (HMC)	HMC
07-T6	135	FLK NN	IB complex	Tuff IB	Contaminated IB
07-T7	135	FLK NN	Below IB	Fine sandstone below IB	High-Al augite
07-T8	135	FLK NN	Below IB	Coarse sandstone below 07-T7	Like IB
07-T9	135	FLK NN	Below IB	Thin sandstone below 07-T8	Between IC, ID
06-T10	FLK NN	FLK NN	IB-IC	Sandstone below IC	HMC
08-T42	145	FLK NN	IC-ID	"Tripartite" sandstone	Like ID
08-T41	145	FLK NN	IB-IC	Coarse sandstone	HMC, minor IB augite
07-T42	137	FLK N	IC-ID	"Tripartite" sandstone	Like ID
07-T40	137	FLK N	IB-IC	Coarse sandstone below IC	HMC, IB, other?
07-T41	137	FLK N	IB-IC	Coarse sandstone below 07-T40	HMC, IB
07-T43	137	FLK N	IB complex	Top of IB complex, sandstone	Like IB
07-T44	137	FLK N	IB complex	Fine ash with clay pellets	Contaminated IB
07-T45	137	FLK N	IB complex	Coarse base of 07-T44	Like IB
10-T40-1	144	FLK N	IB-IC	Fine black ash below IC	Black ash
10-T40-2	147	FLK	IB-IC	Fine black ash below IC	Black ash
08-T54	147	FLK	IB-IC	Sandstone below IC	HMC, IB
08-T55	147	FLK	IB complex	Top of IB "fine caramel" tuff	Like IB
07-T35	138	FLK	ID	Tuff ID top	Like ID
07-T34	138	FLK	ID	Tuff ID base	Like ID
07-T33	138	FLK	IC-ID	"Tripartite" sandstone	Like ID
07-T32	138	FLK	IC	Tuff IC base	Like IC
07-T31	138	FLK	IB-IC	Sandstone with clay below IC	HMC, minor IB augite
07-T30	138	FLK	IB-IC	Sandstone lens below 07-T31	HMC, IB
07-T29	138	FLK	IB-IC	Sandstone above IB	HMC, IB
08-T40	143	Maiko	IB-IC	Sandstone below IC	HMC, IB
08-T39	143	Maiko	IB complex	Crystal rich lapilli tuff	Like IB

Although the admixture of epiclastic particles is obvious from petrographic inspection, it is less clear whether the volcanic particles were derived from direct pyroclastic input or erosion and reworking of volcanics and unconsolidated tephra deposits. Therefore we prefer the term "volcaniclastic sandstone" instead of using "tuffaceous sandstone" (Schmid, 1981), which would include a genetic implication.

The volcaniclastic sandstones were systematically collected (Fig. 2) in one trench from each of FLK (trench 138), FLK N (trench 137), and FLK NN (trench 135), and then in a more targeted fashion in additional trenches from these sites (trenches 144, 145, 147) and from Maiko Gully (trench 143) to the south. Trenches 144 and 147 also exposed a thin, fine-grained black trachyandesitic ash layer not yet identified elsewhere, which was sampled. Examples of detailed trench maps including the stratigraphic positions of individual samples are given in Figures 4 to 6. Figure 7 combines representative measured sections derived from trench backwall maps in a roughly NW-SE trending profile across the FLK area.

Samples were gently disaggregated using a mortar and pestle, sieved, washed in 4% HF for ~1 min in a sonic bath, and rinsed repeatedly. Feldspar, augite, hornblende, and oxide minerals were hand picked and mounted in epoxy for electron probe microanalysis (EPMA). No minimally altered volcanic glass was observed, and titanomagnetite was also absent or sparse in many samples. From volcaniclastic sandstone samples only angular, "fresh" grains were chosen. 10–15 grains of each mineral type were analyzed for each sample (where available) using a Cameca SX51 electron microprobe at the University of Wisconsin-Madison following the methods described in McHenry et al. (2008). Mineral compositions were compared to each other and to a database of Bed I tuff compositions to identify mineral populations related to known tuff markers (McHenry, 2004, 2005; McHenry et al., 2008; McHenry, 2012).

Sedimentary and compositional characteristics of tuffs and volcaniclastic sandstones

The augite, feldspar, and titanomagnetite compositions of all samples analyzed in this study (for compositions represented by at least two grains), including tuffs and volcaniclastic sandstones, are reported in Tables 2–4.

Depositional characteristics of the marker tuffs

Tuff IB in the FLK area is a complex (in terms of facies) stratigraphic unit, and is on average 40 cm thick. Closer to its Olmoti volcanic source to the east, it is easily recognizable as an up to 7.6-m-thick succession of pumice-rich pyroclastic flow and minor surge deposits, overlying a thin (1–5 cm) feldspar-rich fallout tuff (McHenry, 2005). In the FLK area Tuff IB is largely reworked, involving only minor "primary" pyroclastic facies. This suggests deposition over a relatively long time period, with the most primary volcanic facies at the base and extensively reworked facies above. Several of the FLK sections (e.g., Fig. 4, Tr 135) show a basal 3–20 cm thick crystal-rich pumiceous waterlaid lapilli-ash tuff, often with intense deformation due to loading. A ~2-cm-thick pumiceous claystone and a succeeding ~4-cm-thick pumiceous lapilli tuff above are only rarely (e.g., Tr 140) developed. Widespread in the FLK area within Tuff IB is a caramel-brown, laminated, waterlaid fallout ash tuff (4–10 cm) with obvious concentrations of very large pumices (up to 15 cm) near the top. The remainder of Tuff IB comprises either another yellowish fallout ash (8–24 cm) unit or coarse, wave-reworked volcaniclastic sandstones (~60 cm), characterized by admixed lacustrine clays, small soft clay clasts, and ostracod and snail shells (e.g., Tr. 135). This latter unit contains evidence of at least one phase of channeling and deposition of an internal olive waxy lacustrine claystone (see Stollhofen et al. (2008b) for a discussion of waxy (lacustrine) vs. earthy (wetland) claystones at Olduvai). The Tuff IB top surface, in many places rooted and/or deformed by animal trampling, is finally covered by olive waxy lacustrine claystones.

Tuff IC is present in all trenches measured, and of a relatively uniform 20–35 cm thickness. Although in many cases Tuff IC appears as a massive gray to beige-gray colored single unit on first sight, a detailed inspection often reveals a division into up to three subunits. At FLK S three low-angle cross-bedded, coarse ash tuff units are developed, each 7–15 cm thick with a hummocky top. The lowermost of these

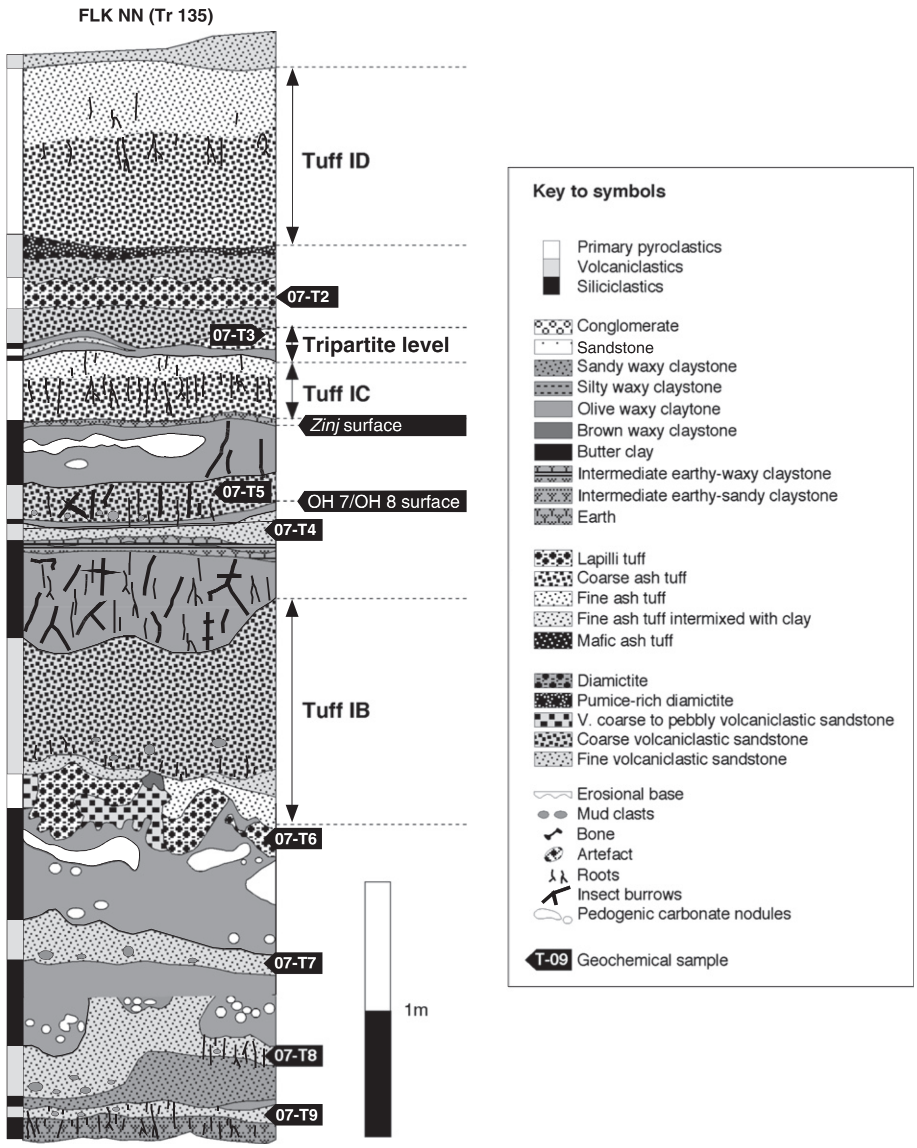

Figure 4. Measured section of Trench 135 (FLK NN) exposing the Tuff IB to Tuff ID interval (left) and key to symbols (right). See Fig. 2 for location of trench. Note the bar to the left of the measured section labeling primary pyroclastic, volcaniclastic and siliciclastic units.

units is confined to a NE-SW incised channel and has a 1–2 cm pumice-lapilli-bearing, feldspar and augite crystal-rich base. Also in the FLK S area (Tr 149) this lowermost unit contains imprints of in situ subaerial parts of subvertical sedges that are bent/inclined westward, suggesting tractional currents during Tuff IC emplacement. This is taken as evidence for deposition of Tuff IC by successive westwardly travelling very dilute surges. Such interpretation also fits with the observation of plant stems at the base of Tuff IC, observed at Tr 147 (FLK) and Tr 149 (FLK S) all subparallel aligned 26° and 40° (NE-SW).

Elsewhere however (e.g., FLK NN, Tr. 134), Tuff IC contains abundant, regularly-spaced subvertical sedge imprints with rooted bases, originating in earthy lithologies underlying Tuff IC. This is taken as evidence that ash fallout mantled existing vegetation and favored its in situ pristine preservation. As within the surge-dominated succession, Tuff IC commonly develops a two- to threefold subdivision but involves textures that support a fallout origin: An initial 1–7 cm thick, pumice lapilli-bearing crystal-rich coarse ash layer (e.g., FLK, Tr 138) is succeeded by a faintly laminated to almost massive, graded coarse to fine ash tuff layer 9–15 cm thick. This succession is then overlain by a crystal-poor fine ash tuff, 7–12 cm thick with a rooted top.

Tuff ID is characterized by 1–3 normally grain-size-graded beige lapilli to ash-lapilli tuff units. Although some exposures in the more eastern parts of Olduvai Gorge show a massive, matrix-supported texture, typical of more viscous pyroclastic flows, the presence of plane lamination, low-angle cross-bedding and relatively constant thicknesses in the FLK area suggests deposition by more dilute, low-viscosity pyroclastic flows and surges there. In places (e.g., Maiko Gully), two flow units are developed, separated by a thin (<2 cm) fine fallout ash, draping over underlying topography. FLK S (Tr. 149) provides a key section, with the Tuff ID succession infilling a shallow (<15 cm), NE-SW (055°) trending channel. A total of eight subunits are developed there with a cumulative thickness of 70 cm. The Tuff ID section is initiated by a yellowish low-angle cross-bedded fine ash surge, 2–7 cm thick, bearing abundant sedge stem fragments up to 20 cm in length and plant leaves. Most of the plant remnants are concentrated at the base of the surge layer showing preferred NNW-SSE to NE-SW alignment. In a few cases, inclined subaerial parts of in situ sedge columns register a northwestward transport direction for the surge. Succeeding units are made up of yellowish to violet gray, plane laminated coarse ash tuffs and pumiceous ash-lapilli tuffs, interpreted as dilute pyroclastic flow and ash-cloud surge deposits.

https://doi.org/10.1016/j.yqres.2013.05.006 Published online by Cambridge University Press

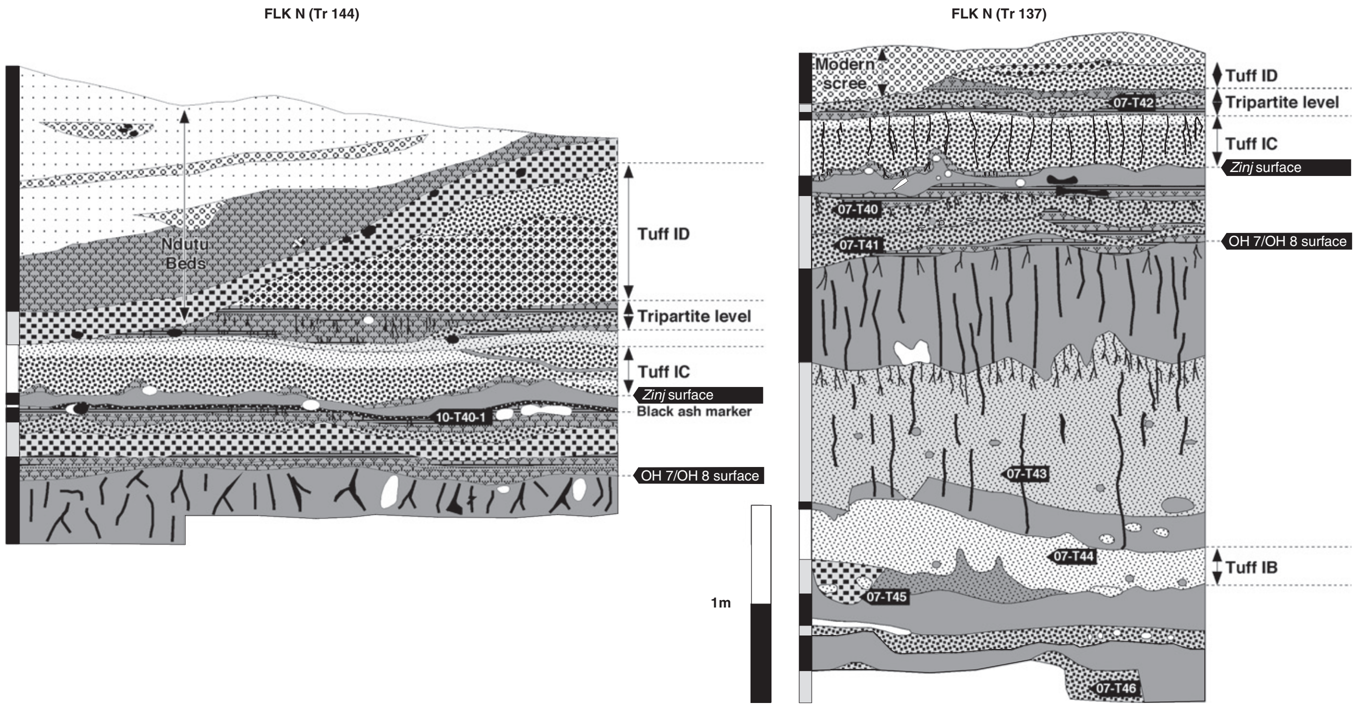

Figure 5. Measured Tuff IB to Tuff ID sections of Trench 144 (left) and Trench 137 (right) at FLK N. See Fig. 2 for location of trenches and Fig. 4 for explanation of symbols.

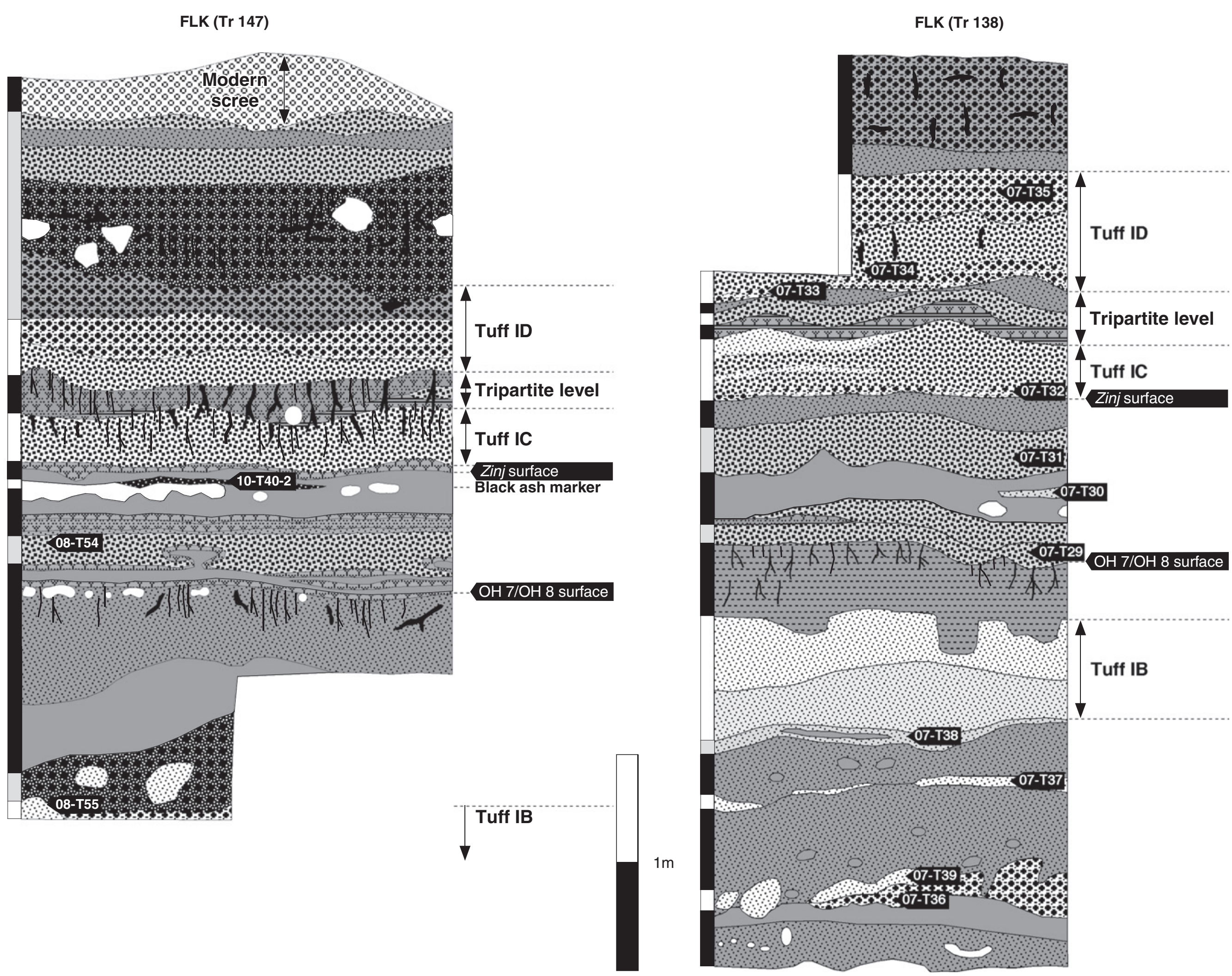

Figure 6. Measured Tuff IB to Tuff ID sections of Trench 147 (left) and Trench 138 (right) at FLK. See Fig. 2 for location of trenches and Fig. 4 for explanation of symbols.

https://doi.org/10.1016/j.yqres.2013.05.006 Published online by Cambridge University Press

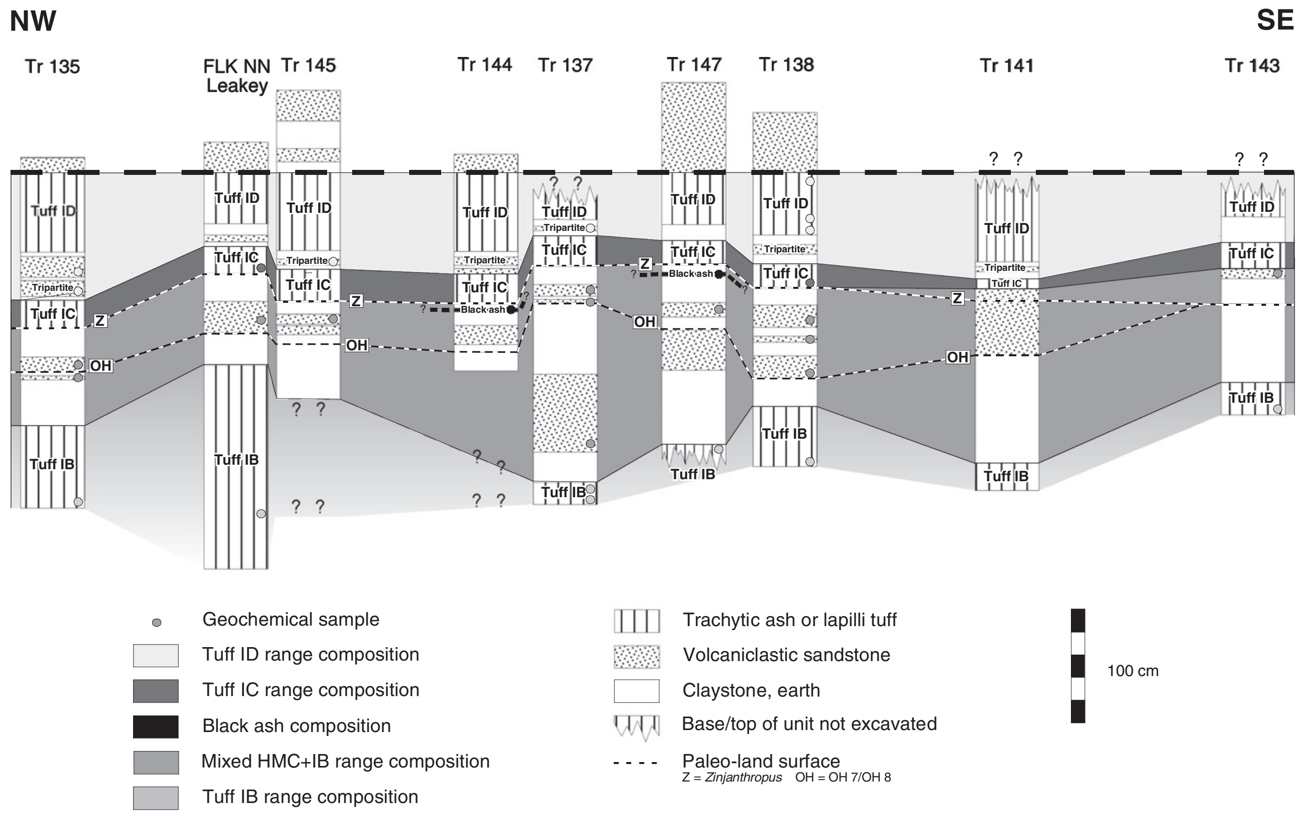

Figure 7. NW-SE cross-section of the FLK NN to FLK S area (c. 500 m) illustrating the application of geochemical stratigraphy of selected grain separates to characterize particular tephrostratigraphic intervals. HMC = "High-Mg Compositional zone." Lateral distances not to scale; see Fig. 2 map for actual trench positions.

Tuff ID sits upon an unconformity throughout the FLK area, which explains how a subaerial tuff can sit upon lacustrine claystone. Although not pronounced in this area, the sub-ID erosional surface does cut down into the top of and through Tuff IC at the nearby HWK W site.

At least one sample of each marker tuff with "primary" depositional characteristics was collected and analyzed as a part of this project, to ensure that the interval had been properly identified. No glass is preserved in the FLK area tuffs due to alteration to clay and zeolite minerals (McHenry, 2009), but feldspar, augite, and (where preserved) titanomagnetite phenocrysts appear to retain their original compositions and can therefore be used for within-basin identification and correlation (Fig. 8).

Marker tuff compositions

As portrayed, Tuff IB is complex and widely contaminated by admixture of non-juvenile components in the FLK area, consistent with the observations of McHenry (2004). Uncontaminated Tuff IB signatures (devoid of feldspar, augite, or titanomagnetite grains inconsistent with IB geochemical compositions) were identified at Maiko Gully (trench 143, sample 08-T39), at FLK N (trench 137, sample 07-T45), and FLK (trench 147, sample 08-T55), representing "primary" pyroclastic deposits. Tuff IB samples from other sites showed some contamination by non-IB mineral compositions. Tuff IC was only analyzed for FLK (trench 138, sample 07-T32) but it should be noted that the "geochemical type" sample for Tuff IC (McHenry, 2005) was collected from the site of the original Leakey trench at FLK NN (Hay, 1976: Locality 45b). Tuff ID was sampled (coarse base and finer top) at FLK (trench 138, samples 07-T34 and 07-T35). Tuffs IC and ID were identified on the basis of their stratigraphic position, their characteristic sedimentary textures and phenocryst assemblages in all other trenches but not analyzed geochemically.

Depositional characteristics of volcaniclastic sandstones

Thin tabular to flat lenticular, fine to medium-grained moderately sorted volcaniclastic sandstones occur at various levels between Tuffs IB and ID. One of such widespread semi-tabular units (referred to by Leakey, 1971 as the "tripartite" level) lies between Tuffs IC and ID (Figs. 4 to 6). Volcaniclastic sandstones vary in thickness between trenches and even across the back and side walls of an individual trench. Based on their thickness, geometry, frequent erosional base contacts, mud clasts and the common association with lacustrine, olive waxy and earthy (wetland) claystones, we interpret prevailing deposition by flood and crevasse splay processes in a vegetated river-fed floodplain/wetland setting (cf. Blumenschine et al., 2012a). Mineral grains show minimal abrasion and rounding, suggesting an originally pyroclastic derivation and minimal recycling. Feldspar, augite, and titanomagnetite dominate these mineral populations, reflecting an overall mineral assemblage comparable to those of the surrounding tuffs. Tables 2–4 summarize the average mineral compositions of the volcaniclastic sandstones.

Compositions of volcaniclastic sandstones between Tuffs IB and IC

Tuffs IB, IC, and ID were definitively identified in FLK area trenches by comparing their mineral compositions to the Bed I tuff composition database of McHenry (2004, 2005, 2012). The volcaniclastic sandstones show more variable mineral assemblages, as expected for redeposited pyroclastic material (Figs. 9, 10). Some of the mineral geochemistries from the sandstones between Tuffs IB and IC do appear to mirror a Tuff IB component (as expected, since unconsolidated Tuff IB material would have been widely available for transport and redeposition), but most also include new mineral compositions not previously observed in any primary Olduvai tuff. This new composition is consistent for all sandstones sampled in the FLK/FLK N/FLK NN area between Tuff Markers IB and IC. It includes augites high in Al, Mg and Ti and low in

https://doi.org/10.1016/j.yqres.2013.05.006 Published online by Cambridge University Press

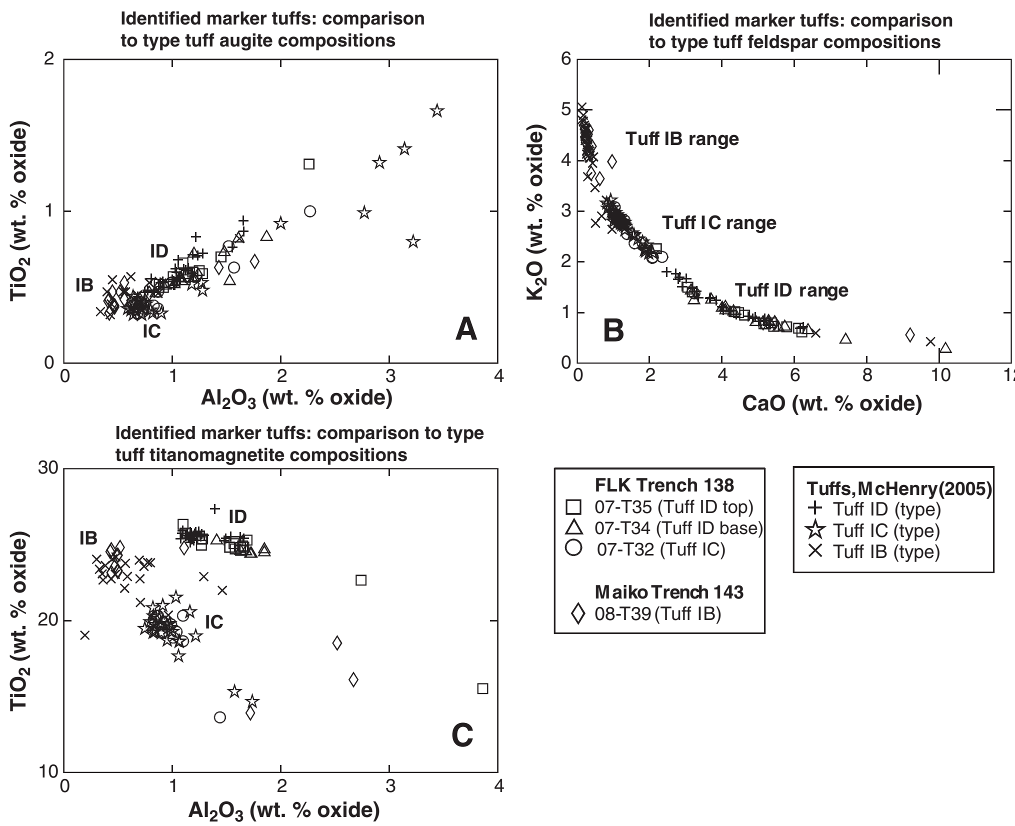

Figure 8. Augite, feldspar, and titanomagnetite compositions for Tuffs IB, IC, and ID from their geochemical type localities (data from McHenry, 2005) compared to Tuffs IB, IC, and ID as identified in the trenches in this study. The tuffs sampled in these trenches were properly identified, matching up in stratigraphic position, mineral assemblage, phenocryst composition, and general appearance/thickness and volcanic facies.

Fe compared to the remaining Bed I tuffs (Fig. 10B; McHenry, 2005; McHenry et al., 2008; McHenry, 2012), anorthoclase similar to Tuff IB but slightly enriched in K (Fig. 10C), and titanomagnetite with high Mg and Al (Fig. 10A). This assemblage is easily distinguishable from the other Bed I tuffs across all three minerals used (Fig. 8, Upper Bed I tuff compositions available in McHenry, 2005, 2012; Lower Bed I tuff compositions available in McHenry et al., 2008), and consistent between trenches and samples of volcaniclastic sandstones of the Tuff IB to IC range in the entire FLK area. Sandstones in this interval do not contain mineral grains consistent with overlying Tuff IC, suggesting that either the appearance of Tuff IC composition detrital material started only with the emplacement of Tuff IC or that IC sits on an erosional surface that removed any early IC equivalent pyroclastic material.

We will refer to this new composition as the "High-Mg Compositional Zone" (HMC) because of elevated Mg concentrations in its augite and titanomagnetite (Fig. 9). Samples 07-T4 and 07-T5 from trench 135 (FLK NN) and sample 06-T10 from the FLK NN Leakey trench have this composition uncontaminated with Tuff IB or other material, and can thus be used as geochemical type samples for the HMC. Other samples from this stratigraphic interval (07-T43 (Tr. 137), 07-T29, 30, and 31 (Tr. 138), and 08-T54 (Tr. 147)) have augite, feldspar, and titanomagnetite that match this composition but also contain some grains of Tuff IB composition, likely from reworking and incorporation of Tuff IB material.

Sample 07-T44 from Trench 137, categorized as "contaminated Tuff IB," is the stratigraphically lowest sample to display this new composition (with a minor population of high-Mg augites, in addition to the expected Tuff IB composition grains), though its feldspar and oxide compositions are consistent with Tuff IB. Minor populations (or single grains) of the HMC augite composition also occur in some overlying units, e.g., Tuff IC at its type section (Fig. 8) and sample 07-T3 above IC in trench 135 (otherwise consistent with Tuff ID compositions). This could result from reworking of small amounts of HMC-dominated sandstones into stratigraphically higher tuffs and sandstones. The incorporation of some grains from underlying sandstones into overlying tephra is not unexpected, especially for tuffs deposited in part as pyroclastic surges.

Compositions of the "tripartite" volcaniclastic sandstone between Tuffs IC and ID

The "tripartite" volcaniclastic sandstone is named from the FLK NN trench map of Leakey, 1971. As the name suggests it is a thin sandstone unit "sandwiched" between two lacustrine claystone beds. The tripartite sandstone sits between Tuffs IC and ID and is similar to overlying Tuff ID in augite, feldspar, and titanomagnetite across all five samples analyzed from four trenches in FLK, FLK N, and FLK NN. For plagioclase feldspar, Tuff ID has more grains in the lower CaO range but the overlap is sufficient to render correlation based on this minor difference unreliable (Fig. 9D).

A significant time gap existed between the deposition of the tripartite sandstone and the subsequent emplacement of Tuff ID. The intervening claystone indicates a lake transgression, followed by lake withdrawal sufficient to generate the subaerial erosion surface on which the subaerial pyroclastic flow of Tuff ID sits (cf. erosion surfaces described by Stanistreet, 2012). Both features imply a significant passage of time from decades to centuries.

Thus the appearance of Tuff ID composition in volcaniclastic sandstones between Tuffs IC and ID suggests that the volcanic source of Tuff ID supplied material to the Olduvai Basin for a considerable time prior to the emplacement of the Tuff ID marker unit and that admixture of sedimentary detritus from other sources initially diluted the Tuff ID source fingerprint to form volcaniclastic sandstones.

https://doi.org/10.1016/j.yqres.2013.05.006 Published online by Cambridge University Press

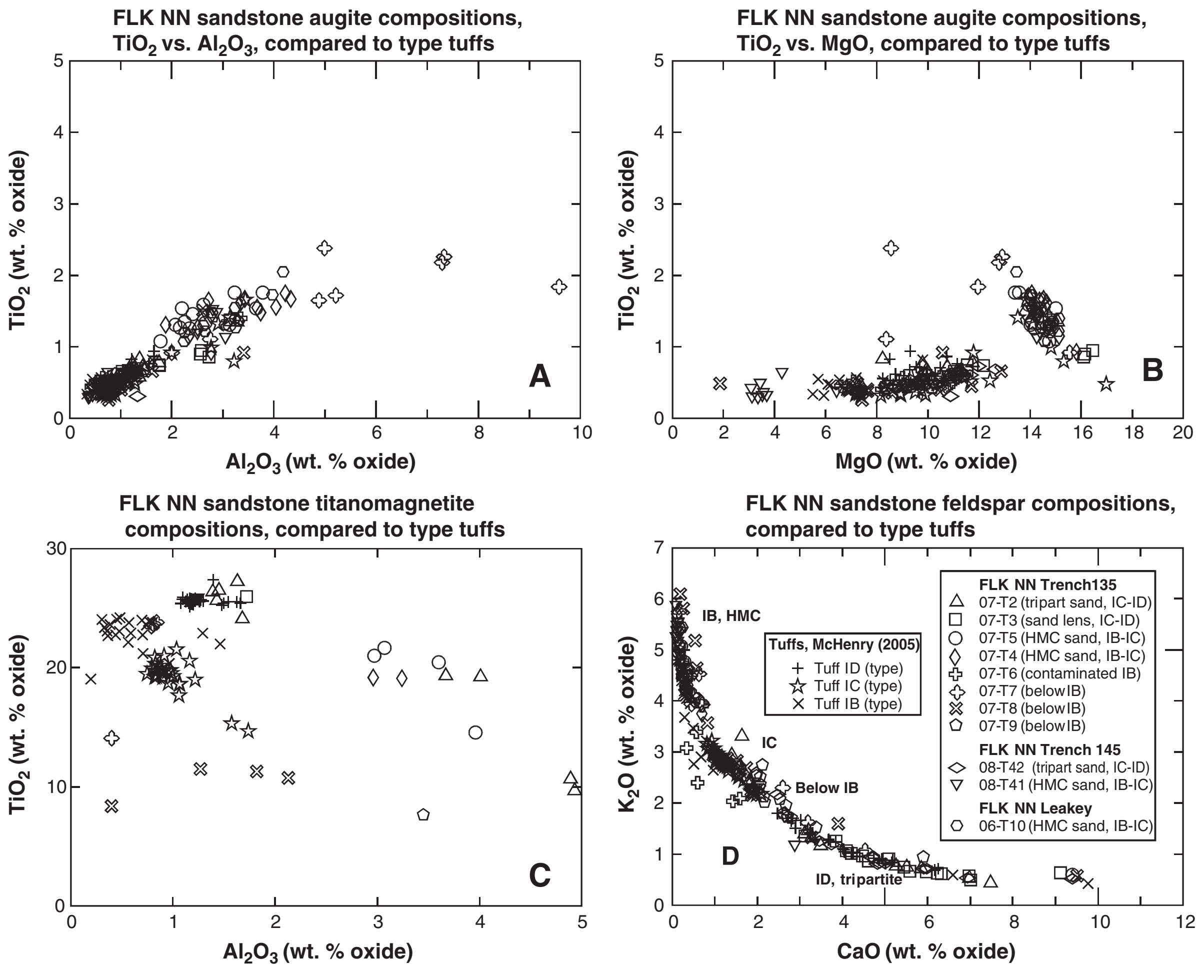

Figure 9. Augite, feldspar, and titanomagnetite compositions for the FLK NN (trenches 135, 145, and FLK NN Leakey) sandstones, compared to the "type" tuffs. For all three minerals, sandstones between Tuffs IC and ID resemble Tuff ID in composition. A and B. Augite. Many sandstones between Tuffs IB and IC fall into a high-Ti, high-Al, high-Mg population distinct from the tuffs, representing a new composition referred to as "High-Mg Compositional zone" (or HMC). Some also fall into the Tuff IB composition range, likely reflecting the incorporation of Tuff IB-derived grains into overlying sandstones. C. Titanomagnetite was rarely preserved in FLK NN sandstones. Where preserved, HMC titanomagnetite has higher Al_2O_3 values than the Bed I tuffs. D. Feldspar. The HMC feldspar composition overlaps Tuff IB, with some grains at slightly higher K_2O concentrations.

However, since no Tuff ID composition material is found below IC, this composition could still restrict sediment samples to a narrow stratigraphic interval. It is also surprising that Tuff IC composition minerals do not appear in sandstones directly above it. A possible explanation for this feature might be that Tuff IC was emplaced very rapidly by only a few volcanic pulses and that environmental conditions, such as the lacustrine transgression that capped Tuff IC with a waxy claystone unit, favored in situ preservation of IC tephra with no obvious reworking of pyroclastic material following Tuff IC emplacement.

The fine black ash tuff marker

The fine black trachyandesitic ash tuff has been identified and sampled in trenches 144 (Fig. 5: 10-T40-1) and 147 (Fig. 6: 10-T40-2) slightly below Tuff IC at both FLK and FLK N. It forms a thin (0.5–1.0 cm) normally grain-size graded tabular to flat lenticular unit draping over the underlying topography which suggests a distal fallout origin. Burial of the ash by lacustrine claystones at trench localities 144 and 147 records localized "quiescent" environmental conditions favoring ash preservation.

This black ash is compositionally distinct from all of the other tuffs and sandstones analyzed in this study. Its augites in particular show higher concentrations of TiO_2 and Al_2O_3 compared to all other samples analyzed (Fig. 10D), and its feldspar compositions fall between Tuffs IB and IC in terms of their K_2O and CaO content (Fig. 10E). No unaltered titanomagnetite phenocrysts were recovered. In the absence of glass or bulk geochemical data, its trachyandesitic nature was determined based on its mineral assemblage dominated by alkali feldspar and sodic plagioclase with minor augite. Its extremely high Al augite composition is well outside the range of any previously analyzed Bed I tuff. Thus, the fine black ash appears to be the product of a different and as of yet unidentified and likely more distant volcanic source. If recognized more broadly, this ash could serve as a useful additional marker to pinpoint the lateral equivalents of both the *Zinjanthropus* and OH 7/OH 8 land surfaces.

Discussion

Tracing the Zinjanthropus and OH 7/OH 8 land surfaces

At FLK, the *Zinjanthropus* land surface (FLK level 22) produced a rich assemblage of fossils (3510 larger mammal fossils) and Oldowan stone artifacts (2566: Leakey, 1971). The same surface is correlated to nearby FLK NN Level 1, another site excavated by Leakey that contained scattered artifacts and less abundant faunal remains (Leakey, 1971; Blumenschine et al., 2012b). The OH 7/OH 8 land surface, at a lower level (level 3) within the same FLK NN excavation, produced a large assemblage of vertebrate fossils (Leakey, 1971),

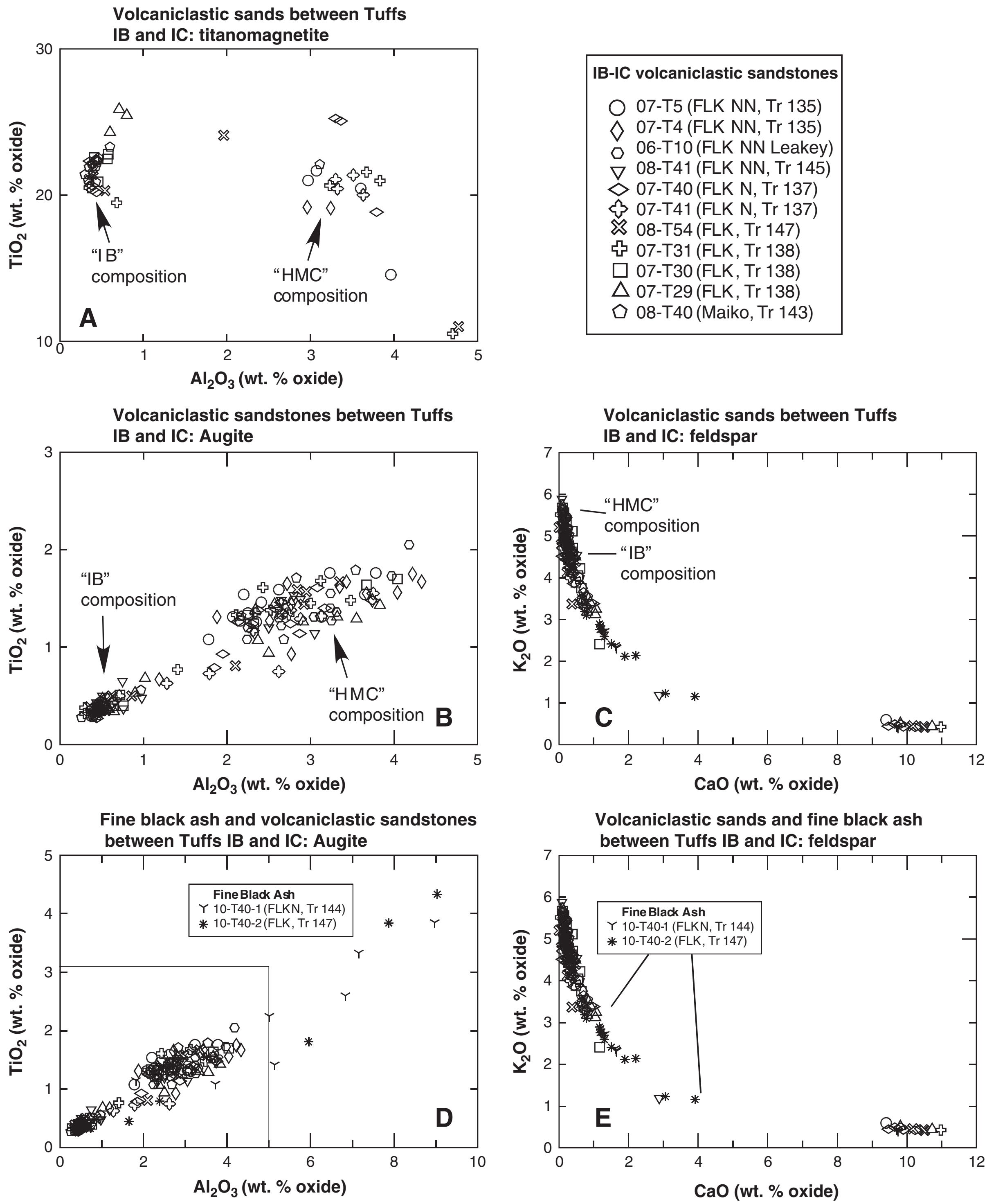

Figure 10. Titanomagnetite, augite, and feldspar compositions from the sandstones between Tuffs IB and IC for all trenches sampled for FLK NN, FLK N, and FLK. A. Titanomagnetite compositions fall into two compositional ranges, one of which overlaps with Tuff IB and the other associated with the HMC composition. B. Augite phenocrysts (TiO_2 vs. Al_2O_3) fall predominantly into the HMC or Tuff IB compositional ranges. C. Sandstone feldspar compositions (K_2O vs. CaO) overlap with the Tuff IB range, trending towards slightly higher K_2O contents. A second, minor plagioclase composition is present in many samples. D. Sandstone augite phenocrysts (TiO_2 vs. Al_2O_3), compared to augite from the fine black ash. Note the much greater range (towards higher Al and Ti) of the black ash augite; the inset rectangle indicates the range of the data plotted in B. E. Sandstone feldspar compositions (K_2O vs. CaO), compared to feldspar from the fine black ash. The black ash feldspar is higher in CaO and lower in K_2O than the sandstones.

including OH 7 and OH 8. Our work traces these land surfaces between the two sites and further south in the FLK area (e.g., Blumenschine et al., 2012a; Stanistreet, 2012). Tuff IC sits directly upon the *Zinjanthropus* land surface and the very rapid emplacement of this tuff undoubtedly contributed to the widespread preservation and burial of this largely in situ assemblage.

The *Zinjanthropus* land surface is an erosional surface incised after a withdrawal of the paleolake to the west and associated base-level fall. The incision cuts deeper in some places than others; there are units below Tuff IC (and the *Zinj* land surface) at FLK that are completely cut out at FLK N and FLK NN, which complicates simple lithostratigraphic correlation between sites (e.g., Blumenschine et

Table 2
Tuff and volcaniclastic sandstone augite compositions as determined by EPMA.

Sample	Pop	n	SiO_2	TiO_2	Al_2O_3	FeO	MnO	MgO	CaO	Na_2O	Sum
Trench 135, FLK NN											
07-T2		14	51.06	0.64	1.22	15.16	0.75	10.25	20.71	0.52	100.29
StDev			0.55	0.10	0.27	1.73	0.08	1.24	0.32	0.08	0.52
07-T3	1	6	51.60	0.60	1.05	12.96	0.77	10.97	20.92	0.49	99.32
StDev			0.41	0.06	0.07	0.40	0.07	0.40	0.17	0.08	0.52
07-T3	2	4	51.67	1.02	2.75	7.34	0.14	15.86	20.40	0.46	99.79
StDev			0.48	0.24	0.27	0.82	0.04	0.76	0.85	0.04	0.47
07-T3	3	2	51.08	0.74	1.76	11.62	0.72	11.86	20.72	0.57	99.15
07-T5		13	51.00	1.43	2.64	8.60	0.21	14.28	19.98	0.45	98.60
StDev			0.64	0.20	0.63	0.68	0.06	0.49	0.91	0.05	0.42
07-T4		14	50.56	1.41	3.07	8.66	0.24	14.20	20.20	0.47	98.85
StDev			0.66	0.31	0.92	1.72	0.19	1.32	0.72	0.08	0.47
07-T6		12	52.03	0.50	0.64	14.20	1.13	9.18	19.70	0.68	98.08
StDev			0.56	0.05	0.10	1.41	0.17	1.37	0.25	0.06	0.56
07-T7	1	6	48.00	1.76	6.05	7.75	0.12	13.60	21.39	0.55	99.22
StDev			1.90	0.48	2.61	1.41	0.08	1.30	1.37	0.19	0.64
07-T7	2	3	48.87	1.30	2.88	13.52	0.40	9.19	21.88	1.23	99.26
StDev			3.04	0.99	2.05	1.11	0.10	1.26	0.52	0.17	0.85
07-T8	1	8	50.31	0.40	0.77	18.85	1.15	7.88	19.98	0.63	99.96
StDev			0.49	0.07	0.07	0.86	0.09	0.66	0.43	0.05	0.56
07-T8	2	3	49.60	1.03	2.55	10.63	0.42	12.59	21.09	0.69	98.60
StDev			1.12	0.44	0.90	1.08	0.26	1.88	0.95	0.47	0.58
08-T8	3	3	51.06	0.44	1.04	14.89	0.90	10.90	20.07	0.46	99.76
StDev			0.17	0.04	0.07	0.68	0.04	0.70	0.26	0.06	0.27
07-T9		5	50.22	0.52	1.09	15.19	0.90	10.01	20.45	0.58	98.95
StDev			0.51	0.10	0.14	0.91	0.13	0.87	0.33	0.08	0.44
Trench 145, FLK NN											
08-T42		13	50.99	0.59	1.20	14.65	0.75	10.99	20.86	0.47	100.50
StDev			0.28	0.11	0.17	1.24	0.09	0.91	0.24	0.14	0.38
08-T41	1	9	48.17	0.40	0.52	23.63	1.16	3.83	19.80	0.93	98.46
StDev			1.49	0.11	0.16	1.70	0.08	1.04	1.00	0.15	1.43
08-T41	2	6	49.84	1.22	2.48	10.75	0.33	13.55	20.12	0.52	98.80
StDev			0.59	0.40	0.76	2.24	0.31	1.64	0.61	0.12	0.53
FLK NN Leakey trench											
06-T10		12	49.73	1.41	3.06	8.96	0.18	14.51	21.04	0.43	99.39
StDev			0.87	0.26	0.61	1.34	0.05	0.49	0.74	0.03	0.93
Trench 137, FLK N											
07-T42	1	12	51.46	0.63	1.26	13.97	0.80	10.36	20.52	0.52	99.51
StDev			0.48	0.10	0.21	1.26	0.13	0.93	0.36	0.08	0.55
07-T42	2	3	51.63	1.14	2.53	8.63	0.20	14.71	19.91	0.38	99.13
StDev			0.13	0.03	0.14	1.48	0.07	0.36	1.13	0.04	0.21
07-T40	1	12	51.48	1.28	2.62	9.46	0.22	13.87	20.08	0.42	99.44
StDev			0.60	0.24	0.55	0.66	0.07	0.28	0.53	0.07	0.31
07-T40	2	8	50.09	0.35	0.47	23.02	1.15	4.04	19.71	0.79	99.62
StDev			0.45	0.06	0.05	1.01	0.09	0.58	0.42	0.14	0.48
07-T41	1	11	49.98	0.40	0.52	22.60	1.16	4.25	19.59	0.82	99.33
StDev			0.55	0.05	0.10	2.20	0.06	1.56	0.25	0.18	0.29
07-T41	2	8	51.63	1.10	2.56	8.31	0.22	14.38	20.62	0.39	99.22
StDev			0.95	0.35	0.77	1.64	0.15	1.07	0.48	0.05	0.39
07-T43	1	12	51.06	0.43	0.53	19.18	1.28	6.89	19.66	0.74	99.78
StDev			0.42	0.04	0.12	1.53	0.18	1.09	0.32	0.12	0.56
07-T43	2	3	51.61	0.79	1.69	12.18	0.65	11.78	20.26	0.49	99.47
StDev			0.31	0.23	0.80	2.07	0.29	1.22	0.66	0.06	0.29
07-T44	1	15	50.70	0.43	0.53	19.34	1.35	6.90	19.41	0.70	99.38
StDev			0.41	0.05	0.11	1.58	0.14	1.16	0.43	0.09	0.48
07-T44	2	3	50.69	1.39	3.48	8.10	0.16	13.94	21.11	0.42	99.29
StDev			2.20	0.35	1.91	1.24	0.03	1.05	0.36	0.09	0.75
07-T45	1	10	50.68	0.41	0.48	20.31	1.37	6.25	19.17	0.82	99.49
StDev			0.29	0.03	0.04	0.96	0.08	0.48	0.44	0.07	0.37
07-T45	2	5	51.78	0.49	0.80	15.07	0.95	10.05	19.92	0.54	99.60
StDev			0.34	0.06	0.21	1.64	0.20	1.09	0.44	0.08	0.27
Trench 144, FLK N											
10-T40-1		7	46.87	2.24	5.52	8.52	0.13	13.54	21.50	0.52	98.83
StDev			3.05	1.09	2.37	1.75	0.07	1.71	1.19	0.19	1.27
Trench 147, FLK											
08-T54	1	7	49.79	0.40	0.53	24.20	1.12	4.55	19.78	0.88	101.25
StDev			0.44	0.08	0.17	2.66	0.13	1.73	0.40	0.20	0.47
08-T54	2	6	50.82	1.40	2.80	9.83	0.22	14.71	20.34	0.47	100.60
StDev			0.69	0.31	0.41	1.56	0.06	0.78	0.77	0.10	0.35
08-T55		7	50.14	0.47	0.51	19.01	1.35	7.73	19.33	0.72	99.27
StDev			0.72	0.04	0.11	1.30	0.10	1.13	0.45	0.11	0.73

(continued on next page)

https://doi.org/10.1016/j.yqres.2013.05.006 Published online by Cambridge University Press

Table 2 (*continued*)

Sample	Pop	n	SiO_2	TiO_2	Al_2O_3	FeO	MnO	MgO	CaO	Na_2O	Sum
10-T40-2	1	4	49.70	1.15	3.37	6.18	0.11	16.25	21.91	0.37	99.04
Trench 147, FLK											
StDev			2.24	0.63	1.88	1.38	0.02	1.73	0.29	0.08	1.68
10-T40-2	2	2	42.95	4.08	8.45	9.20	0.11	11.72	22.02	0.46	98.99
Trench 138, FLK											
07-T35		12	49.86	0.65	1.23	13.96	0.61	10.46	21.49	0.50	98.83
StDev			0.65	0.21	0.36	0.86	0.09	0.79	0.46	0.06	0.75
07-T34		11	50.63	0.62	1.26	12.91	0.54	11.48	21.59	0.50	99.68
StDev			0.58	0.13	0.32	2.77	0.14	1.84	0.49	0.09	0.42
07-T33		17	50.95	0.64	1.24	13.62	0.74	10.92	20.91	0.50	99.64
StDev			0.53	0.12	0.22	1.16	0.07	0.84	0.35	0.12	0.84
07-T32	1	10	51.61	0.39	0.78	15.15	1.11	8.17	20.14	0.69	97.88
StDev			0.42	0.06	0.10	1.28	0.12	1.17	0.49	0.08	0.67
07-T32	2	3	52.44	0.80	1.79	9.19	0.61	13.55	19.92	0.78	99.18
StDev			0.29	0.19	0.42	1.86	0.13	1.48	0.22	0.18	0.55
07-T31	1	10	51.52	1.38	2.58	8.53	0.24	14.06	20.39	0.50	99.16
StDev			0.57	0.24	0.57	0.90	0.12	0.74	0.75	0.09	0.72
07-T31	2	4	50.28	0.34	0.37	20.76	1.12	3.35	19.76	0.96	96.92
StDev			0.40	0.03	0.09	1.12	0.06	0.77	0.25	0.12	0.88
07-T30	1	9	50.52	0.41	0.56	18.89	1.14	5.06	20.13	0.74	97.42
StDev			0.59	0.04	0.11	1.97	0.14	1.78	0.41	0.13	0.86
07-T30	2	4	51.72	1.47	3.07	7.31	0.20	14.23	20.76	0.46	99.16
StDev			0.91	0.23	0.92	1.05	0.03	0.47	0.75	0.03	0.08
07-T29	1	8	51.00	1.27	2.92	6.87	0.14	14.86	20.76	0.42	98.24
StDev			0.54	0.18	0.58	0.91	0.06	0.67	0.69	0.04	0.60
07-T29	2	5	50.19	0.47	0.73	16.59	0.92	6.83	20.62	0.60	97.11
StDev			0.32	0.14	0.22	0.90	0.06	0.75	0.19	0.06	0.49
Trench 143, Maiko Gully											
08-T40	1	11	48.87	0.34	0.45	23.89	1.17	3.87	19.72	0.87	99.19
StDev			0.33	0.05	0.07	0.90	0.13	0.58	0.43	0.08	0.67
08-T40	2	4	49.50	1.47	2.80	9.95	0.21	14.43	19.40	0.48	98.26
StDev			0.81	0.33	0.56	0.86	0.05	0.67	1.55	0.04	0.16
08-T39	1	14	49.81	0.43	0.57	20.36	1.34	6.78	19.35	0.84	99.48
StDev			0.71	0.07	0.22	1.39	0.15	0.97	0.42	0.10	1.08
08-T39	2	2	50.74	0.65	1.59	12.13	0.58	12.71	20.47	0.51	99.37

Pop = population, n = number of grains analyzed.

al., 2012a; Stanistreet, 2012). The composition of individual mineral grains separated from successive volcaniclastic sandstones collected between Tuffs IB and IC from one trench has so far been insufficient to “fingerprint” the individual sandstones. Thus, in the absence of the thin, black ash tuff, other stratigraphic techniques need to be applied in order to identify the erosive downcutting of the *Zinjanthropus* land surface. However, the presence of a sandstone of primarily HMC composition in augite, feldspar, and titanomagnetite would constrain the stratigraphic interval to between Tuffs IB and IC. Future work will seek potential correlatives of this sandstone composition in the eastern gorge and western paleolacustrine deposits, where this interval may be more difficult to identify because of the local absence of Tuff IC (McHenry, 2005, 2012).

This work supports the conclusion that the *Zinjanthropus* level of FLK (with its abundant lithic and faunal remains, including the actual *P. boisei* skull) is stratigraphically distinct from the OH 7/OH 8 level at FLK NN, (which includes the type specimen for *H. habilis*). The *Zinjanthropus* level is also identified at FLK NN (equivalent of Leakey's (1971) FLK NN level 1), which contains some lithic and faunal remains. The proximity of these two sites, in both time and space, is a classic example of the co-existence of multiple hominin species. The compositionally based volcaniclastic sandstone correlations build on the detailed lithostratigraphic correlations presented by Blumenschine et al. (2012a) and Stanistreet (2012).

Conclusions

1. In this example from Olduvai, volcaniclastic sandstones are considered not only as reworked deposits of underlying tephra but also as potential archives of geochemically unique pyroclastic grain compositions not preserved as “primary” tuffs within the Olduvai basin.
2. Such compositionally unique assemblages allow for higher stratigraphic resolution than possible solely using established Marker Tuff tephrostratigraphy, and can help test lithostratigraphic correlations. The HMC compositional assemblage, found in greatest abundance in volcaniclastic sandstones between Tuffs IB and IC, could help identify this interval in areas where the marker tuffs are not preserved.
3. A new trachyandesitic tuff composition has been identified between Tuff Markers IB and IC and contrasts compositionally with all other known Lower and Upper Bed I tuffs.
4. In the case of the volcaniclastic sandstones of the tripartite level of FLK NN and its lateral equivalents between Tuffs IC and ID, their mineralogical similarity to overlying Tuff ID reveals that Tuff ID composition pyroclastic material was supplied to the Olduvai basin long before the emplacement of the Tuff ID unit proper.
5. The defined “volcaniclastic sandstone grain fingerprints” potentially provide an additional basis for the development of a Tuff IB to Tuff ID stratigraphic framework, particularly in those cases where conventional tephrostratigraphic marker tuffs are lacking or only discontinuously preserved due to erosion, e.g., the eastern, western, and lacustrine parts of the Olduvai basin (cf. Hay, 1976; Blumenschine et al., 2003), helping to trace the archeologically important *Zinjanthropus* and OH 7/OH 8 levels.

Acknowledgments

We would like to thank the Tanzania Commission for Science and Technology and the Tanzania Antiquities Department for granting us permission to conduct research at Olduvai Gorge. Robert Blumenschine,

Table 3
Tuff and volcaniclastic sandstone feldspar compositions as determined by EPMA.

Sample	Pop	n	SiO_2	Al_2O_3	FeO	CaO	Na_2O	K_2O	BaO	Sum
Trench 135, FLK NN										
07-T2	1	5	61.01	25.01	0.29	6.22	7.55	0.64	0.34	100.97
StDev			0.98	0.75	0.07	0.96	0.39	0.15	0.14	0.55
07-T2	2	5	66.88	20.70	0.23	1.37	8.64	3.09	0.37	101.28
StDev			0.52	0.55	0.06	0.55	0.18	0.62	0.18	0.22
07-T2	3	4	64.67	22.78	0.20	3.27	8.67	1.34	0.26	101.19
StDev			0.37	0.35	0.06	0.16	0.07	0.13	0.11	0.31
07-T3		14	61.84	24.04	0.22	5.21	7.95	0.85	0.25	100.29
StDev			1.55	1.02	0.05	1.20	0.44	0.26	0.20	0.45
07-T5		7	66.98	20.44	0.26	1.53	7.82	4.30	0.17	101.50
StDev			4.13	2.92	0.14	3.47	0.84	1.67	0.09	0.38
07-T4		6	68.65	19.61	0.25	0.29	8.01	4.85	0.16	101.77
StDev			0.24	0.39	0.07	0.22	0.42	0.72	0.08	0.16
07-T6		13	67.33	19.94	0.28	0.64	8.38	3.62	0.46	100.61
StDev			1.08	0.70	0.05	0.53	0.91	1.05	0.31	0.47
07-T7	1	8	67.08	19.66	0.29	0.51	8.03	4.35	0.46	100.38
StDev			0.43	0.28	0.12	0.17	0.36	0.61	0.27	0.51
07-T7	2	7	63.57	21.47	0.25	2.77	8.46	1.73	0.36	98.60
StDev			2.17	1.41	0.16	1.08	0.68	0.91	0.19	3.07
07-T8	1	10	65.43	21.21	0.21	1.99	8.52	2.42	0.48	100.26
StDev			1.30	0.91	0.07	0.92	0.26	0.65	0.18	0.51
07-T8	2	4	67.15	19.45	0.26	0.39	7.54	5.43	0.23	100.44
StDev			0.56	0.17	0.05	0.20	0.30	0.65	0.09	0.59
07-T9	1	13	64.60	21.48	0.27	2.40	8.52	2.13	0.48	99.89
StDev			0.75	0.61	0.32	0.42	0.19	0.39	0.19	0.46
07-T9	2	2	61.01	24.32	0.26	5.32	7.65	0.95	0.20	99.68
Trench 145, FLK NN										
08-T42	1	9	61.93	23.69	0.27	5.05	7.80	0.87	0.29	99.90
StDev			1.25	1.00	0.03	1.10	0.44	0.23	0.11	0.33
08-T42	2	2	65.35	20.71	0.24	1.89	8.57	2.48	0.51	99.76
08-T41		14	67.50	19.28	0.29	0.16	7.72	5.31	0.00	100.26
StDev			0.37	0.20	0.07	0.11	0.26	0.32	0.16	0.36
FLK NN Leakey trench										
06-T10		5	65.41	19.11	0.27	0.30	7.96	4.93	0.04	98.01
StDev			1.10	0.27	0.07	0.08	0.12	0.46	0.06	1.45
Trench 137, FLK N										
07-T42		14	61.15	24.18	0.25	4.93	7.63	0.77	0.26	99.17
StDev			0.77	0.64	0.04	0.66	0.28	0.12	0.12	0.50
07-T40	1	10	67.00	19.64	0.28	0.38	7.85	4.20	0.24	99.59
StDev			0.81	0.32	0.06	0.28	0.29	0.52	0.19	0.80
07-T40	2		55.48	27.82	0.50	9.81	5.23	0.46	0.05	99.30
StDev		5	0.21	0.23	0.03	0.28	0.16	0.04	0.10	0.33
07-T41		15	66.92	19.61	0.27	0.31	7.82	4.44	0.16	99.53
StDev			0.40	0.33	0.04	0.18	0.29	0.54	0.10	0.51
07-T43		13	66.78	19.64	0.31	0.33	7.92	4.06	0.29	99.34
StDev			0.51	0.35	0.04	0.15	0.23	0.38	0.19	0.49
07-T44	1	10	66.34	19.87	0.31	0.49	8.03	3.85	0.26	99.14
StDev			0.60	0.47	0.07	0.44	0.27	0.69	0.17	0.51
07-T44	2	3	60.61	24.71	0.29	5.49	7.48	0.56	0.28	99.42
StDev			0.73	0.51	0.01	0.52	0.39	0.08	0.11	0.20
StDev			0.32	0.21	0.06	0.08	0.26	0.41	0.16	0.57
07-T45	2	3	58.30	26.09	0.38	7.38	6.51	0.56	0.12	99.31
StDev			3.32	2.48	0.13	2.80	1.48	0.14	0.16	0.45
Trench 144, FLK N										
10-T40-1	1	7	65.84	19.88	0.28	0.26	8.01	4.78	0.15	99.20
StDev			0.90	0.29	0.04	0.04	0.14	0.19	0.06	1.31
10-T40-1	1	7	64.58	20.65	0.24	1.17	8.40	2.93	0.52	98.50
StDev			1.03	0.54	0.05	0.51	0.24	0.66	0.18	1.17
10-T40-1	3	2	54.26	27.64	0.50	9.72	5.36	0.43	0.01	97.88
Trench 147, FLK										
10-T40-2	1	11	64.35	20.76	0.28	1.32	8.51	2.68	0.44	98.35
StDev			0.90	0.50	0.04	0.43	0.22	0.35	0.15	0.78
10-T40-2	2	3	62.28	23.30	0.21	3.53	8.60	0.87	0.27	99.05
StDev			0.26	0.76	0.08	0.43	0.41	0.56	0.14	1.22
10-T40-2	3	2	65.56	19.59	0.28	0.30	8.09	4.35	0.27	98.42
08-T54	1	12	68.23	19.54	0.29	0.27	7.99	4.64	0.21	101.16
StDev			0.53	0.33	0.05	0.13	0.24	0.55	0.17	0.75
08-T54	2	3	56.33	28.00	0.53	10.38	5.19	0.44	0.06	100.92
StDev			0.24	0.03	0.08	0.18	0.07	0.02	0.08	0.15
08-T55		15	67.21	19.31	0.33	0.25	8.19	4.55	0.28	100.11

(continued on next page)

https://doi.org/10.1016/j.yqres.2013.05.006 Published online by Cambridge University Press

Table 3 (*continued*)

Sample	Pop	n	SiO_2	Al_2O_3	FeO	CaO	Na_2O	K_2O	BaO	Sum
StDev			0.56	0.26	0.05	0.08	0.19	0.41	0.16	0.84
Trench 138, FLK										
07-T35	1	13	62.21	23.73	0.23	4.71	7.90	1.02	0.28	100.07
StDev			1.58	1.16	0.08	1.24	0.43	0.46	0.15	0.41
07-T34		15	61.18	24.27	0.28	5.16	7.62	0.90	0.20	99.57
StDev			2.50	1.59	0.10	1.82	0.87	0.31	0.15	0.72
07-T33	1	14	61.48	23.81	0.28	4.90	7.92	0.94	0.29	99.62
StDev			1.13	1.11	0.06	1.04	0.41	0.41	0.16	1.12
07-T33	2	2	56.96	26.96	0.49	8.95	5.94	0.64	0.09	99.95
07-T32		12	65.94	20.99	0.27	1.68	8.82	2.46	0.53	100.68
StDev			0.88	0.70	0.08	0.67	0.19	0.49	0.27	0.48
07-T31		12	67.80	19.38	0.26	0.17	7.94	5.26	0.16	100.90
StDev			0.30	0.23	0.10	0.08	0.29	0.44	0.10	0.35
07-T30		12	67.21	19.73	0.23	0.47	8.34	4.41	0.33	100.68
StDev			0.54	0.26	0.07	0.27	0.45	0.82	0.20	0.36
07-T29	1	9	67.07	20.14	0.20	0.72	8.57	3.67	0.39	100.75
StDev			0.44	0.33	0.03	0.28	0.35	0.54	0.19	0.60
07-T29	2	2	55.37	27.86	0.39	10.26	5.53	0.48	0.08	99.96
Trench 143, Maiko Gully										
08-T40		15	67.23	19.66	0.31	0.36	8.15	4.62	0.15	100.48
StDev			0.50	0.38	0.10	0.23	0.35	0.67	0.17	0.46
08-T39	1	11	67.40	19.48	0.34	0.39	8.20	4.23	0.23	100.28
StDev			0.77	0.27	0.23	0.22	0.29	0.34	0.23	0.77
08-T39	1	3	59.69	25.03	0.34	6.60	7.17	0.72	0.09	99.63
StDev			2.56	1.58	0.11	2.26	1.08	0.13	0.21	0.24

Pop = population, n = number of grains analyzed.

Fidelis Masao, Jackson Njau, Rosa Albert, Marion Bamford, and other collaborators from the Olduvai Landscape Paleoanthropology Project (OLAPP) and the Olduvai Geochronology and Archaeology Project (OGAP) provided invaluable support in the field, and Kiel Finn and John Fournelle provided much appreciated laboratory assistance. Research was sponsored by grants of the National Science Foundation (BCS-0852292), the L.S.B. Leakey Foundation, the University of Wisconsin- Milwaukee Research Growth Initiative, DFG and DAAD, the Wenner-Gren Foundation for Anthropological Research, the National Geographic Committee for Research and Exploration, and the Center for Human Evolutionary Studies, Rutgers University.

References

Albert, R.M., Bamford, M.K., 2012. Vegetation during deposition of uppermost Bed I including Tuff IF at Olduvai Gorge, Tanzania, based on phytoliths and plant remains. Journal of Human Evolution 63, 342–350.

Alloway, B.V., Larsen, G., Lowe, D.J., Shane, P.A.R., Westgate, J.A., 2007. Tephrochronology. In: Elias, S.A. (Ed.), Encyclopaedia of Quaternary Science. Elsevier, London, pp. 2869–2898.

Ashley, G.M., Barboni, D., Dominguez-Rodrigo, M., Bunn, H.T., Mabulla, A.Z.P., Diez-Martin, F., Barba, R., Baquedano, E., 2010a. A spring and wooded habitat at FLK Zinj and their relevance to origins of human behavior. Quaternary Research 74, 304–314.

Ashley, G.M., Barboni, D., Dominguez-Rodrigo, M., Bunn, H.T., Mabulla, A.Z.P., Diez-Martin, Barba, R., Baquedano, E., 2010b. Paleoenvironmental and paleoecological reconstruction of a freshwater oasis in savannah grassland at FLK North, Olduvai Gorge, Tanzania. Quaternary Research 74, 333–343.

Bamford, M.K., 2012. Fossil sedges, macroplants and roots from Olduvai Gorge. Journal of Human Evolution 63, 351–363.

Bamford, M.K., Albert, R.M., Cabanes, D., 2006. Assessment of the lowermost Bed II Plio-Pleistocene vegetation in the eastern palaeolake margin of Olduvai Gorge (Tanzania) and preliminary results from macroplant fossil remains and phytoliths. Quaternary International 148, 95–112.

Bamford, M.K., Stanistreet, I.G., Stollhofen, H., Albert, R.M., 2008. Late Pliocene grassland from Olduvai Gorge, Tanzania. Palaeogeography, Palaeoclimatology, Palaeoecology 257, 280–293.

Blumenschine, R.J., Peters, C.R., Masao, F.T., Clarke, R.J., Deino, A.L., Hay, R.L., Swisher, C.C., Stanistreet, I.G., Ashley, G.M., McHenry, L.J., Sikes, N.E., Van der Merwe, N.J., Tactikos, J.C., Cushing, A.E., Deocampo, D.M., Njau, J.K., Ebert, J.I., 2003. Late Pliocene *Homo* and hominid land use from western Olduvai Gorge, Tanzania. Science 299, 1217–1221.

Blumenschine, R.J., Stanistreet, I.G., Njau, J.K., Bamford, M.K., Masao, F.T., Albert, R.M., Stollhofen, H., Andrews, P., Prassack, K.A., McHenry, L.J., Fernández-Jalvo, Y., Camilli, E.L., Ebert, J.I., 2012a. Environments and hominin activities across the FLK Peninsula during *Zinjanthropus* times (1.84 Ma), Olduvai Gorge, Tanzania. Journal of Human Evolution 63, 364–383.

Blumenschine, R.J., Masao, F.T., Stollhofen, H., Stanistreet, I.G., Bamford, M.K., Albert, R.M., Njau, J.K., Prassack, K.A., 2012b. Landscape distribution of Oldowan stone artifact assemblages across the fault compartments of the eastern Olduvai Lake Basin during early lowermost Bed II times. Journal of Human Evolution 63, 384–394.

Cronin, S.J., Wallace, R.C., Neall, V.E., 1996. Sourcing and identifying andesitic tephras using major oxide titanomagnetite and hornblende chemistry, Egmont volcano and Tongariro Volcanic Centre, New Zealand. Bulletin of Volcanology 58, 33–40.

Deino, A.L., 2012. $^{40}Ar/^{39}Ar$ dating of Bed I, Olduvai Gorge, Tanzania, and the chronology of early Pleistocene climate change. Journal of Human Evolution 63, 252–273.

Froggatt, P.C., 1992. Standardization of the chemical analysis of tephra deposits. Report of the ICCT working group. Quaternary International 13–14, 93–96.

Hay, R.L., 1976. Geology of the Olduvai Gorge: A Study of Sedimentation in a Semiarid Basin. University of California Press, Berkeley.

Leakey, M.D., 1971. Olduvai Gorge— Excavation in Beds I and II 1960–1963, 3. Cambridge University Press, Cambridge.

Lowe, D.J., 2011. Tephrochronology and its application: a review. Quaternary Geochronology 6, 107–153.

Matsu'ura, T., Miyagi, I., Furusawa, A., 2011. Late Quaternary cryptotephra detection and correlation in loess in northeastern Japan using cummingtonite geochemistry. Quaternary Research 75, 624–635.

McHenry, L.J., 2004. Characterization and Correlation of Altered Plio-Pleistocene Tephra Using a "Multiple Technique" Approach: Case Study at Olduvai Gorge, Tanzania. Ph.D. thesis Rutgers University, New Brunswick, NJ.

McHenry, L.J., 2005. Phenocryst composition as a tool for correlating fresh and altered tephra, Bed I, Olduvai Gorge, Tanzania. Stratigraphy 2, 101–115.

McHenry, L.J., 2009. Element mobility during zeolitic and argillic alteration of volcanic ash in a closed-basin lacustrine environment: case study Olduvai Gorge, Tanzania. Chemical Geology 265, 540–552.

McHenry, L.J., 2012. A revised stratigraphic framework for Olduvai Gorge Bed I based on tuff geochemistry. Journal of Human Evolution 63, 284–299.

McHenry, L.J., Mollel, G.M., Swisher III, C.C., 2008. Compositional and textural correlations between Olduvai Gorge Bed I tephra and volcanic sources in the Ngorongoro Volcanic Highlands, Tanzania. Quaternary International 178, 306–319.

Njau, J.K., Blumenschine, R.J., 2012. Crocodylian and mammalian carnivore feeding traces on hominid fossils from FLK 22 and FLK NN 3, Plio-Pleistocene, Olduvai Gorge, Tanzania. Journal of Human Evolution 63, 408–417.

Pante, M.C., Blumenschine, R.J., Capaldo, S.D., Scott, R.S., 2012. Validation of bone surface modification models for inferring fossil hominin and carnivore feeding interactions, with reapplication to FLK 22, Olduvai Gorge, Tanzania. Journal of Human Evolution 63, 395–407.

Sarna-Wojcicki, A.M., 2000. Tephrochronology. In: Noller, J.S., Sowers, J.M., Lettis, W.R. (Eds.), Quaternary geochronology: methods and applications. AGU Reference Shelf, vol. 4. American Geophysical Union, Washington, DC, pp. 357–377.

Sarna-Wojcicki, A.M., Davis, J.O., 1991. Quaternary tephrochronology. Quaternary Nonglacial Geology: Conterminous U.S. The Geology of North America. Geological Society of America, Boulder, pp. 93–116.

Schmid, R., 1981. Descriptive nomenclature and classification of pyroclastic deposits and fragments: recommendations of the IUGS subcommission on the systematics of igneous rocks. Geology 9, 41–43.

Table 4
Tuff and volcaniclastic sandstone titanomagnetite compositions as determined by EPMA.

Sample	Pop	n	SiO_2	TiO_2	Al_2O_3	FeO	MnO	MgO	CaO	Cr_2O_3	Sum
Trench 135, FLK NN											
07-T2	1	5	0.25	25.95	1.52	63.03	1.32	1.20	0.08	0.05	93.35
StDev			0.32	1.18	0.13	3.24	0.14	0.14	0.09	0.03	2.33
07-T2	2	2	0.11	19.27	3.84	65.89	0.42	4.87	0.05	0.44	94.89
07-T2	3	2	0.08	10.16	4.91	74.02	0.34	3.13	0.02	0.52	93.17
07-T5		4	0.12	19.42	3.40	65.29	0.42	3.82	0.20	0.83	93.49
StDev			0.03	3.28	0.47	3.55	0.08	0.30	0.17	0.46	0.42
07-T4		2	0.10	19.14	3.10	65.16	0.38	3.62	0.39	0.71	92.60
07-T5		3	0.13	21.04	3.21	63.53	0.44	3.92	0.27	0.82	93.37
StDev			0.03	0.61	0.34	0.59	0.09	0.27	0.14	0.56	0.42
07-T7		4	0.09	10.48	1.41	75.17	1.08	2.17	0.19	0.15	90.71
StDev			0.09	1.43	0.76	1.48	0.24	1.40	0.10	0.23	1.41
07-T8		3	0.11	23.64	0.81	65.88	1.67	0.61	0.14	0.01	92.87
StDev			0.03	0.16	0.03	0.56	0.07	0.03	0.08	0.02	0.39
Trench 137, FLK N											
07-T40	1	4	0.46	20.90	0.41	69.91	1.37	0.23	0.43	0.01	93.72
StDev			0.36	1.02	0.03	3.04	0.03	0.06	0.21	0.01	2.28
07-T40	2	2	0.36	25.07	3.24	58.61	0.37	0.59	0.03	1.47	89.75
07-T41		5	0.41	21.00	2.83	61.17	0.55	3.89	0.40	3.08	93.34
StDev			0.49	0.83	1.37	1.83	0.46	2.00	0.25	1.94	1.59
07-T43		8	0.22	24.88	0.63	63.93	1.74	0.76	0.17	0.01	92.32
StDev			0.08	0.60	0.27	2.59	0.16	0.38	0.13	0.02	2.37
07-T44		13	0.24	25.07	0.81	64.02	1.72	0.92	0.10	0.02	92.87
StDev			0.17	0.42	0.24	1.53	0.17	0.39	0.09	0.02	1.78
07-T45	1	12	0.24	24.21	0.48	66.41	1.80	0.52	0.10	0.00	93.75
StDev			0.13	0.78	0.04	2.32	0.06	0.06	0.06	0.00	1.55
07-T45	2	5	0.18	24.54	1.43	65.57	1.28	1.62	0.12	0.02	94.77
StDev			0.04	0.56	0.32	1.37	0.30	0.19	0.06	0.02	1.33
Trench 147, FLK											
08-T54		6	0.10	19.93	1.40	69.95	1.25	1.14	0.11	N.A.	93.88
StDev			0.03	4.55	1.76	1.63	0.36	1.49	0.14		2.64
Trench 138, FLK											
07-T35		15	0.10	24.33	1.70	67.14	1.09	1.66	0.05	0.07	96.14
StDev			0.02	2.56	0.71	0.80	0.29	0.74	0.04	0.21	1.09
07-T34		7	0.10	24.61	1.70	66.41	1.10	1.63	0.04	0.02	95.60
StDev			0.02	0.30	0.15	1.39	0.06	0.14	0.03	0.02	1.48
07-T33		13	0.09	25.61	1.49	64.29	1.27	1.35	0.05	N.A.	94.13
StDev			0.03	0.54	0.20	1.56	0.07	0.34	0.03		1.77
07-T32		11	0.13	19.11	1.01	71.68	1.43	0.69	0.11	0.02	94.14
StDev			0.04	1.91	0.17	1.96	0.10	0.20	0.19	0.01	1.19
07-T31	1	4	0.14	18.43	3.86	63.81	0.43	3.81	0.31	3.79	93.56
StDev			0.06	5.28	0.62	6.04	0.06	0.73	0.20	1.48	1.33
07-T31	2	2	0.16	19.99	0.51	68.99	0.99	0.54	0.28	0.05	91.48
07-T30		4	0.13	22.19	0.51	68.34	1.40	0.24	0.18	0.03	92.99
StDev			0.06	0.86	0.08	2.10	0.07	0.03	0.22	0.01	1.44
07-T29		3	0.19	25.20	0.70	64.78	1.43	0.39	0.16	0.02	92.84
StDev			0.24	0.82	0.10	0.56	0.07	0.03	0.04	0.03	0.20
Trench 143, Maiko Gully											
08-T40	1	11	0.11	22.01	0.42	68.52	1.45	0.24	0.13	0.01	92.90
StDev			0.04	0.70	0.08	1.44	0.08	0.06	0.14	0.03	1.35
08-T40	2	2	0.08	19.43	4.83	64.56	0.41	3.60	0.00	1.28	94.20
08-T93	1	9	0.11	23.97	0.48	66.51	1.79	0.52	0.11	0.00	93.48
StDev			0.04	0.67	0.03	1.79	0.10	0.06	0.07	0.02	1.26
08-T39	2	3	0.11	16.18	2.30	73.30	0.45	0.29	0.00	0.11	92.75
StDev			0.01	2.30	0.51	2.04	0.21	0.29	0.02	0.03	0.94

Pop = population, n = number of grains analyzed, N.A. = not analyzed.

Stanistreet, I.G., 2012. Fine resolution of early hominin time, Beds I and II, Olduvai Gorge, Tanzania. Journal of Human Evolution 63, 300–308.

Stollhofen, H., Stanistreet, I.G., 2012. Plio-Pleistocene synsedimentary fault compartments, foundation for the eastern Olduvai Basin paleoenvironmental mosaic, Tanzania. Journal of Human Evolution 63, 309–327.

Stollhofen, H., Werner, M., Stanistreet, I.G., Armstrong, R.A., 2008a. Single zircon U/Pb dating of Carboniferous–Permian tuffs, Namibia, and the intercontinental deglaciation cycle framework. In: Fielding, C.R., Frank, T.D., Isbell, J.L. (Eds.), Resolving the Late Paleozoic Ice Age in time and space: Geological Society of America Special Paper 441, pp. 83–96.

Stollhofen, H., Stanistreet, I.G., McHenry, L.J., Mollel, G.F., Blumenschine, R.J., Masao, F.T., 2008b. Fingerprinting facies of the Tuff IF marker, with implications for early hominin paleoecology, Olduvai Gorge, Tanzania. Palaeogeography, Palaeoclimatology, Palaeoecology 259, 382–409.

Tryon, C.A., Logan, M.A.V., Mouralis, D., Kuehn, S., Slimak, L., Balkan-Atlı, N., 2009. Building a tephrostratigraphic framework for the Paleolithic of central Anatolia, Turkey. Journal of Archaeological Science 36, 637–652.

Turner, M.B., Bebbington, M.S., Cronin, S.J., Stewart, R.B., 2009. Merging eruption datasets: building an integrated Holocene eruptive record for Mt Taranaki, New Zealand. Bulletin of Volcanology 71, 903–918.

WoldeGabriel, G., Hart, W.K., Katoh, S., Beyene, Y., Suwa, G., 2005. Correlation of Plio-Pleistocene tephra in Ethiopian and Kenyan rift basins: temporal calibration of geological features and hominid fossil records. Journal of Volcanology and Geothermal Research 147, 81–108.

https://doi.org/10.1016/j.yqres.2013.05.006 Published online by Cambridge University Press